

## Damped harmonic oscillation: Linear or quadratic drag force?

R. Hauko, and R. Repnik

Citation: *American Journal of Physics* **87**, 910 (2019); doi: 10.1119/1.5124978

View online: <https://doi.org/10.1119/1.5124978>

View Table of Contents: <https://aapt.scitation.org/toc/ajp/87/11>

Published by the [American Association of Physics Teachers](#)

---

---

AIP Author Services  
English Language Editing





# Damped harmonic oscillation: Linear or quadratic drag force?

R. Hauko

*Faculty of Mechanical Engineering, University of Maribor, Smetanova 17, SI-2000 Maribor, Slovenia*

R. Repnik

*Faculty of Natural Sciences and Mathematics, University of Maribor, Koroška c. 160, SI-2000 Maribor, Slovenia and Association for Technical Culture of Slovenia, Zaloška c. 65, 1000 Ljubljana, Slovenia*

(Received 17 March 2019; accepted 17 August 2019)

Harmonic oscillation damped by quadratic drag force is rarely found in physics textbooks. We present typical characteristics of the phenomenon and an analytical tool for the experimental determination of the resistance regime. The measurement is simulated using randomly generated amplitudes with different types of statistical and systematic errors. Their impact on the process of distinguishing between the linear and quadratic regimes and on the measured damping parameters is studied. © 2019 American Association of Physics Teachers.

<https://doi.org/10.1119/1.5124978>

## I. INTRODUCTION

When teaching oscillation in physics class, we use the basic laws of mechanics and the principle of energy conservation and prepare connections with quantum mechanics. The understanding of oscillations is the basis for solving engineering problems, as has been shown in a great number of published papers.

Most studies follow a standard pattern that includes a description of a specific experiment with a comparison of the measured quantities and the theoretical model results.<sup>1–6</sup> The most common topic is damped oscillation, with three varieties of energy loss: oscillation with constant drag force (friction) and oscillation with linear or square-velocity-dependent drag force. In most cases, the author(s) assumed that the appropriate form of damping is known.<sup>7–11</sup> Only a few studies differentiate the effects of different regimes based on experimental results.<sup>12–14</sup>

For damping oscillation caused by the surrounding medium (gas, liquid), one can use the calculation of the Reynolds number  $Re$  to theoretically differentiate between two regimes: for  $Re < 1$ , we assume a linear law, for  $Re > 1000$ , a square law, but for the intermediate values, determination of the dominant regime is not unambiguous and depends on the particular situation.<sup>15–18</sup>

In practice, the oscillation is often clearly in one of the defined resistance regimes. In such cases, changing the regime requires a change in the value of  $Re$  of at least 3 orders of magnitude. Thus, in most real systems, by changing the initial amplitudes of the oscillation and the proportional velocity amplitude, the resistance regime does not change. A similar conclusion applies to changing the velocity within a single swing.<sup>19</sup>

Nevertheless, calculating  $Re$  for a simple spring/mass system on an air track is not sufficient to describe the regime: in a common experiment with  $Re \cong 100$ , the decrease in amplitude indicates a linear drag force.<sup>14,20</sup> Therefore, it is useful to have an analytical tool with which we can determine the regime from real experiments and compare results with theoretical assumptions.

Thus, we are interested in the ability to determine the type of velocity-dependent damping by measuring the time-series of the amplitude. For this purpose, we simulated measured amplitudes in both regimes with different types and sizes of measurement errors. For experimental samples, we used random sets, adjusted different theoretical functions, and compared the measured parameters obtained with default values.

Although the concept of measurement (and measurement results) usually refers to a real experiment, in this study, we used it for a set of simulated values. The study described is generalized and not related to any specific type of oscillation, and so the findings can be used on a variety of realistic physical oscillating systems.

## II. ANALYSIS AND RESULTS

A common experimental exercise in high-schools and universities determines the damping coefficient by measuring the time dependence of the oscillation amplitude. In this approach, a viscous drag force and an exponential decrease in the amplitude  $|x_0(t)| = x_0 \exp(-Bt)$  with  $B$  as a damping parameter are assumed.

No current textbooks include oscillation using the square drag law  $|F_d| \propto v^2$ .<sup>21–25</sup> In this case, the equation of motion  $\ddot{x} + dx^2 \cdot \text{Sign}(\dot{x}) + \omega_0^2 x = 0$  cannot be analytically solved, and we have to implement numerical procedures to find approximate solutions. It turns out that the time dependence of the amplitude is in good agreement with the function  $|x_0(t)| = x_0/(1 + Dt)$  (Fig. 1), where  $D = 4dx_0\omega_0/(3\pi)$  is the parameter of quadratic damping.<sup>8</sup> It can be shown that such an oscillation cannot be critically damped or over damped and that the frequency is equal to the frequency of the undamped oscillator.<sup>26</sup> Unlike viscous damping, where the decrease in amplitude is “at all times just like itself,” the decrease depends on the initial distance and the frequency of the oscillation.

Figure 2 shows the time dependence of the relative amplitude  $|x_0(t)|/x_0$  for selected parameters for both regimes. Functions  $Y_1 = e^{-\alpha}$  and  $Y_2 = 1/(1 + \alpha)$  and  $\alpha = Bt$  or  $\alpha = Dt$  present theoretical values. For default values  $B = B_{theo.} = 1 \text{ s}^{-1}$  or  $D = D_{theo.} = 1 \text{ s}^{-1}$ , the values on the x-axis present the time in seconds. In addition, we include random sets of measured values for the same parameters.

The simulated values are generated at intervals  $\Delta\alpha = 0.1$  and are distributed around the theoretical values with a constant absolute (statistical) error  $\sigma = 0.05$ .<sup>27,28</sup> Here,  $\sigma$  is a measurement error, expressed relative to the initial amplitude  $x_0$ . Therefore, we assume that the initial amplitude is measured precisely enough to ignore its error. For the linear drag, additional sets of simulated values for statistical error  $\sigma = 0.03$  and  $\sigma = 0.10$  are shown.

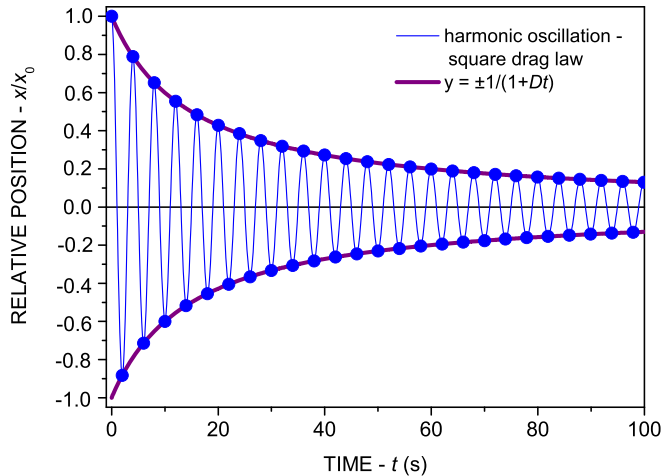


Fig. 1. Theoretical relative position  $x(t)/x_0$  of the damped harmonic oscillator in the case of square drag force (blue) and the adjustment function  $y = \pm 1/(1 + Dt)$  (purple), which describes the time dependence of the relative amplitude,  $d = 0.10 \text{ m}^{-1}$ ,  $\omega_0 = 1.57 \text{ s}^{-1}$ , and  $D = 0.0668 \text{ s}^{-1}$ .

We adapted both one-parameter model functions  $y_1 = e^{-Bt}$  and  $y_2 = 1/(1 + Dt)$  to all simulated measurement sets by gradually integrating additional points at the end of the measurement range  $\alpha$  into the fitting procedure. The measured damping parameters  $B$  and  $D$  (obtained from fitting) were compared with the default theoretical value  $B_{theo.} = 1 \text{ s}^{-1}$  or  $D_{theo.} = 1 \text{ s}^{-1}$  (used in the simulation).

When expanding the measuring range, two criteria were used to determine the correct adjustment function and the corresponding resistance regime:

- (1) Variations of the measured damping coefficient value
- (2) Difference in the quality of the fits

In the case of an appropriate fitting function ( $y_1$  or  $y_2$ ), the value of the measured damping parameter  $B$  or  $D$  approaches the default theoretical value  $1 \text{ s}^{-1}$  with increasing  $\alpha$ . Otherwise, the value is changed approximately linearly by increasing the interval (Fig. 3). The convergence is reasonable, as one can better detect the validity of the fitting function applied on a larger interval. Interestingly, variation of the derived parameter is

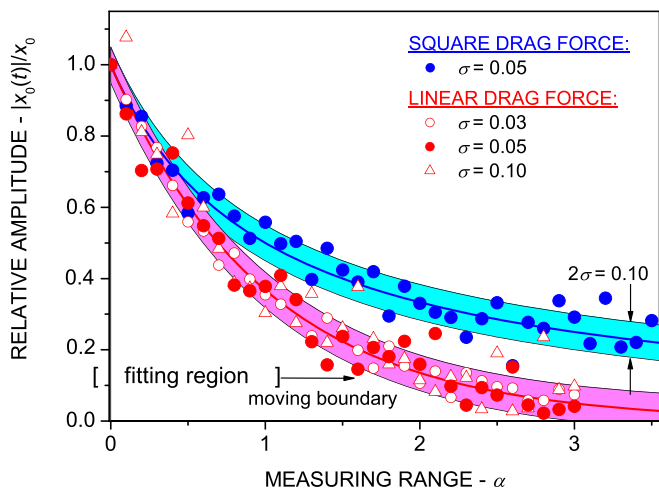


Fig. 2. Theoretical relative amplitude for the linear drag law (red line) and square drag law (blue line) together with randomly generated values (symbols) at different statistical error rates. The areas for  $\pm\sigma = \pm 0.05$  around the theoretical functions are shaded with the corresponding colors.

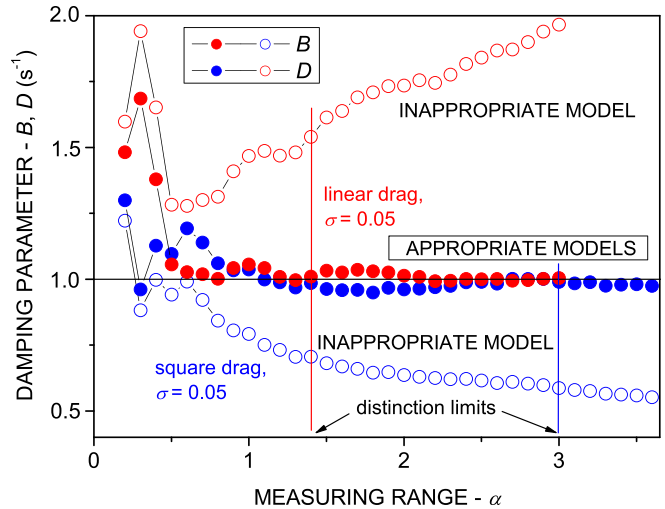


Fig. 3. The values of the measured damping parameter  $B$  or  $D$ , depending on the measuring range  $\alpha$  for both simulated regimes with  $\sigma = 0.05$ . At a short measuring range, the values fluctuate randomly. For models that adequately describe the resistance regime (filled circles), the parameter values converge to the default theoretical value  $1 \text{ s}^{-1}$ , while in inadequate models (empty circles), the values at a large measuring range change approximately linearly. The lower limits of the measuring range for a reliable determination of the drag regime are set to  $\alpha = 1.4$  for the linear drag law (red line) and  $\alpha = 3.0$  for the square drag law (blue line). When approaching this range, the damping parameter for the appropriate fitting function varies more slowly than that for the inappropriate function, which provides a reliable distinction.

almost independent of the statistical error value  $\sigma$ . Therefore, even for relatively large measuring errors, we can distinguish both regimes by observing the convergence of the damping parameters  $B$  and  $D$ . Nevertheless, the measured range must be long enough that the amplitude decreases to at least  $\sim 25\%$  of the initial value ( $\alpha = 1.4$  for the linear law and  $\alpha = 3.0$  for the square law) (Table I).

The quality of the fit is estimated by the root-mean-square error RMSE.<sup>27–29</sup> With  $\Delta(\text{RMSE})$ , we indicate the difference in the RMSE value obtained by fitting the same dataset with two different fitting functions. When using the appropriate fitting function, RMSE values converge roughly to the value  $\sigma$ , which is usually  $\sigma \geq 0.01$  for real experiments. Therefore, we set the value  $\Delta(\text{RMSE}) = 0.01$  as the resolution limit for the difference in the quality of the fits. Minimum relative amplitude for reliable determination of the regime according to the  $\Delta(\text{RMSE})$  criterion depends slightly on the  $\sigma$  value (Table I). In general, the impact of random errors in the data simulation on  $\Delta(\text{RMSE})$  becomes negligible when the amplitude of the oscillation drops to  $\sim 25\%$  of the initial value. Here,  $\Delta(\text{RMSE}) > 0.01$  and increases monotonically, which enables a reliable determination of the regime (Figs. 4 and 5).

Table I. Approximate upper limit values of relative amplitude  $|x_0(t)|/x_0$  for reliable determination of the regime according to both criteria for both resistance regimes at different statistical errors  $\sigma$ .

Criterion	Resist. regime	$\sigma = 0.03$	$\sigma = 0.05$	$\sigma = 0.10$
$B$ and $D$ convergence	LIN.	0.27	0.25	0.22
	QUAD.	0.26	0.25	0.24
$\Delta(\text{RMSE})$	LIN.	0.50	0.22	0.15
	QUAD.	0.35	0.27	0.23

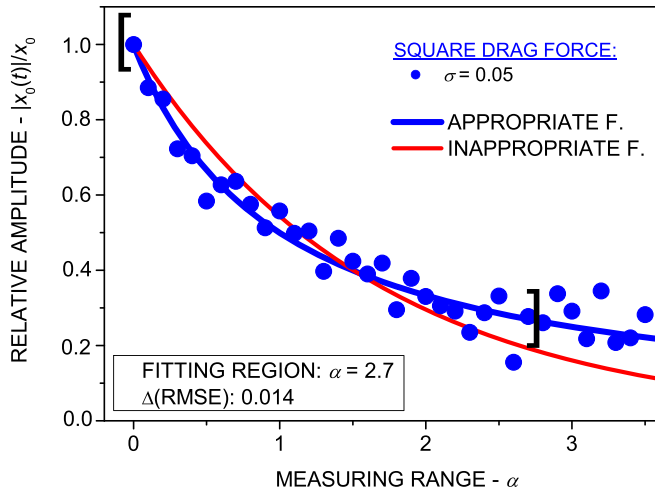


Fig. 4. Simulated measurement set for the square drag law with  $\sigma = 0.05$  and both fitting functions at  $\alpha = 2.7$  ( $|x_0(t)|/x_0 = 0.27$ ). The appropriate fitting function follows the measured points outside the included range; consequently, with additional expansion of the fitting range, the measured damping parameter changes only slightly (Fig. 3). In addition, the fit with the appropriate function is better according to the visual criterion, since the function follows the generated points in the entire fitting region equally well.

Fitting functions can be expanded by introducing additional parameters  $A$  or  $C$ :  $y_1 = Ae^{-Bt}$  or  $y_2 = C/(1 + Dt)$ . While using relative amplitudes, this extension is reasonable only when the error of the initial amplitude  $x_0$  is not negligible. For our generated sets, additional flexibility of the fitting functions improves the modelling error only slightly. Furthermore, the ability to distinguish both model functions remains the same and the calculated value of the parameter  $B$  or  $D$  differs from the simulated value  $1 \text{ s}^{-1}$  even more. By introducing additional parameters  $A$  and  $C$  for  $\sigma = 0.05$  and the largest measuring range, the value  $B$  changes from 1.004 to 0.966 and value  $D$  changes from 0.982 to 0.952 in the case of appropriate fitting function, meaning that by introducing  $A$  or  $C$ , the discrepancy increases from 0.4% to 3.4% and from 1.8% to 4.8%.

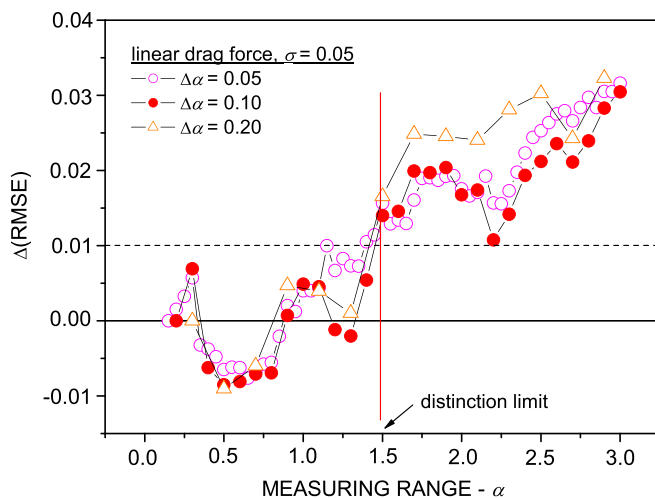


Fig. 5. Differences in fit quality  $\Delta(\text{RMSE})$  between appropriate and inappropriate fitting functions at different numbers of measuring points (simulated amplitudes) within the same measuring range  $\alpha$  for the linear drag law and statistical error  $\sigma = 0.05$ . For reliable regime determination, a measuring range  $\alpha \sim 1.5$  is needed for all three measurement simulation densities. From here on,  $\Delta(\text{RMSE}) > 0.01$ , and it increases almost monotonically.

When measuring the damped oscillation amplitude, the number of measurement points is limited by the ratio between the degree of attenuation and the frequency and by the ability to measure small amplitudes. At a sufficiently high oscillation frequency, the change of the step in the simulation (the density of simulated amplitudes) is equivalent to changing the drag rate in a real experiment. Figure 5 shows the effect of the number of simulated measuring points on the difference in the quality of both fits  $\Delta(\text{RMSE})$ . The simulated data correspond to the linear drag at  $\sigma = 0.05$ . At  $\alpha = 3.0$ , for steps  $\Delta\alpha = 0.05, 0.1$ , and  $0.2$ , we obtain 60, 30, and 15 measuring points, respectively. We can see that the change in the number of measuring points inside the same measuring range does not significantly affect the ability to identify the appropriate fitting function. In all cases, we need a measuring range  $\alpha$  around 1.5 ( $|x_0(t)|/x_0 = 0.22$ ). The same applies to the values  $B$  or  $D$  obtained by fitting. Therefore, the ability to identify the correct regime is roughly independent of the degree of damping; it depends only on the dynamic range of data. The latter is also true for the square law.

At this point, we can summarize the findings on the experimental determination of the resistance regime in the case of random errors:

- (1) Both of the analyzed criteria are robust and roughly independent of the statistical error rates.
- (2) For reliable determination, the measured relative amplitude has to be  $\sim 0.25$ .
- (3) The use of relative amplitudes and one-parameter fitting functions is recommended in the analysis. The introduction of an additional parameter does not affect the ability to determine the regime, but it may increase the error of the measured damping parameter.
- (4) The ability to determine the resistance regime does not depend on the degree of damping.

Furthermore, we include three types of systematic errors in simulated measurement sets:

- (1) Equilibrium position error—the measured equilibrium position differs by constant value  $E$  from the true equilibrium position, which gives the relative error  $\delta = E/x_0$ .
- (2) Normalization error—the measured initial amplitude differs by constant value  $F$  from the true initial amplitude, which gives the relative error  $\delta = F/x_0$ .
- (3) Constant error—all measured amplitudes differ by constant value  $G$  from the true amplitude values, which gives the relative error  $\delta = G/x_0$ .

Figure 6 shows the influence of these systematic errors in the case of an ideal example of viscous damping in the absence of random errors. For demonstration purposes, the magnitudes of systematic errors are larger than is usual in real experiments. Additionally, they are selected in such a way as to increase the probability of incorrect identification of the regime. For the square law, we obtain similar characteristics.

Figures 7 and 8 present the impact of the constant error on the parameter  $B$  or  $D$  and on the difference in the quality of fits  $\Delta(\text{RMSE})$  by varying the range  $\alpha$ , respectively. The simulated data correspond to linear drag at  $\sigma = 0.05$  and the one-parameter fitting functions are used. We notice that for  $\delta > 0.1$ , only detailed analysis of the convergence of parameters  $B$  or  $D$  over the entire range  $\alpha$  enables the determination of the damping regime. The latter is no longer possible according to the  $\Delta(\text{RMSE})$  criterion. The obtained value of parameter  $B$  at  $\delta = 0.10$  and  $\sigma = 0.05$  is  $\sim 20\%$  below the true value. Similar findings are true for the square drag law.

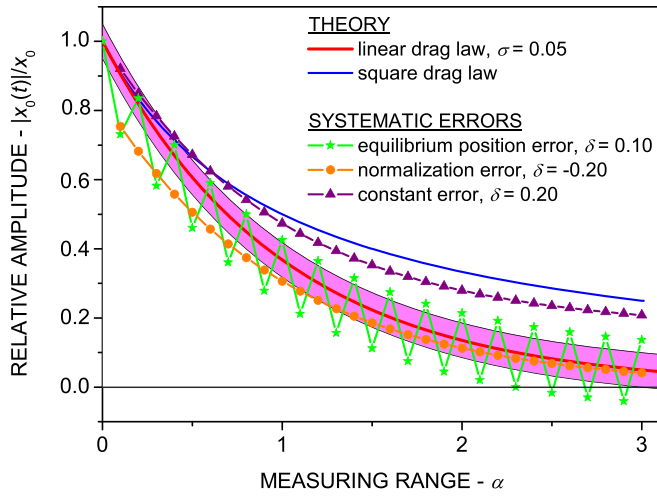


Fig. 6. The influence of systematic errors (connected symbols) on the theoretical relative amplitude for the linear drag law (red line). For normalization and constant error, the amplitude curves are similar to the theoretical curve for the square drag law (blue line), which makes it difficult to determine the resistance regime. For comparison, the shaded area  $\pm\sigma = \pm 0.05$  around the linear drag curve is shown.

Table II shows the impact of systematic errors for  $\delta \sim 0.1$  on the ability to experimentally determine the resistance regime for both criteria by using one-parameter fitting functions. The measured values of the damping parameter  $B$  or  $D$  are also shown for the appropriate fitting functions and the large measuring range value  $\alpha$ . All characteristics are similar for both damping regimes. Slow convergence of the measured damping coefficient  $B$  or  $D$  and the low  $\Delta(\text{RMSE})$  value signal the need to extend both fitting functions with additional parameters.

The normalization error can be detected and compensated for by introducing the additional parameters  $A$  or  $C$  to fitting functions  $y_1 = Ae^{-Bt}$  or  $y_2 = C/(1 + Dt)$ . For an appropriate fitting function, the fit quality improves considerably, the

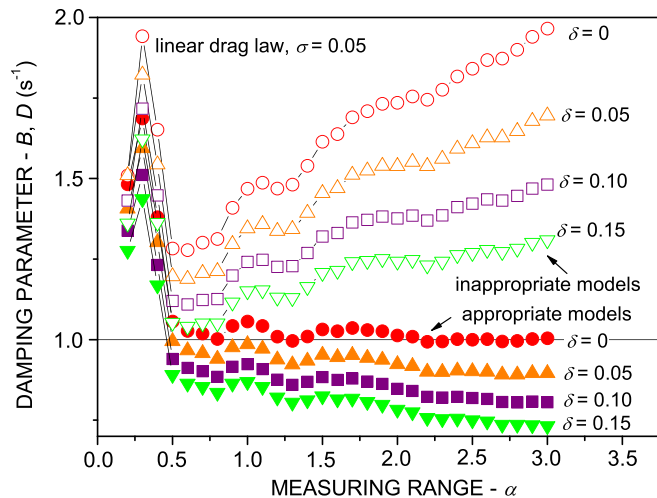


Fig. 7. The values of the damping parameter  $B$  (filled symbols) or  $D$  (empty symbols) depending on the measuring range  $\alpha$  for different values of constant systematic error  $\delta$ . The generated measurement sets correspond to the linear drag law at  $\sigma = 0.05$ . For  $\delta > 0.1$ , only detailed analysis of the variation of parameters  $B$  and  $D$  over the entire range  $\alpha$  enables the determination of the damping regime. Over the large measuring range, the measured damping parameter  $B$  (from appropriate models) differs greatly from the default value  $B_{theo.} = 1 \text{ s}^{-1}$ .

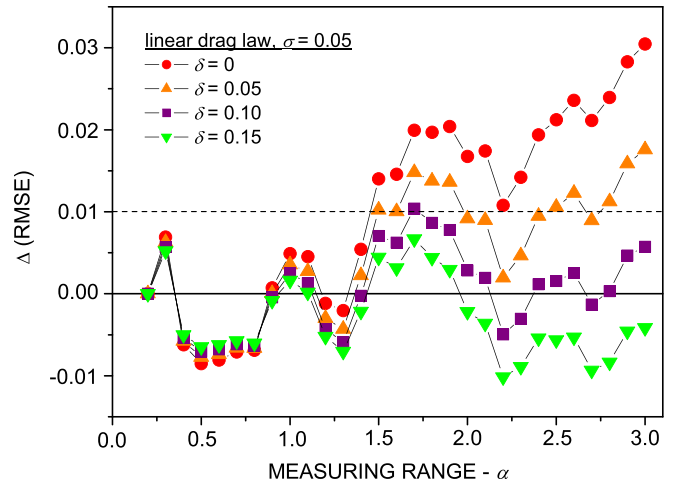


Fig. 8. Differences in fit quality  $\Delta(\text{RMSE})$  between appropriate and inappropriate fitting functions at different values of the constant systematic error  $\delta$ , depending on the measuring range  $\alpha$ . The generated measurement sets correspond to the linear drag law at  $\sigma = 0.05$ . For  $\delta > 0.1$ , a combination of two types of errors enables a determination of the resistance regime according to the  $\Delta(\text{RMSE})$  criterion.

parameter  $A$  or  $C$  compensates for the normalization error, and the damping parameter  $B$  or  $D$  remains in the proximity of  $1 \text{ s}^{-1}$  (true value). For an inadequate fitting function, the quality of the fit is not improved.

In the case of constant error, the use of absolute amplitudes is more effective than the use of relative (normalized) amplitudes. This enables us to detect and compensate for the error directly by introducing a third parameter in the form of an additive constant to the fitting function  $y_1 = Ae^{-Bt} + H$  or  $y_2 = C/(1 + Dt) + I$ . Conversely, if all measured amplitudes have the same relative error, the normalization process removes this error.

### III. CONCLUSIONS

In our analysis, we show that the ability to determine the proper drag regime and the damping coefficient depends primarily on the size of the dynamic range of measurements, that is, on the ability to measure small amplitudes. In real experiments, it is therefore preferable to choose a large initial amplitude. However, we must keep in mind that it is necessary to remain within the linear-dependence range between distance and acceleration, which is a condition for harmonic oscillation.

We show that in the initial phase of an analysis, it is recommended to use relative amplitudes and two one-parameter model functions. The criteria for determining the regime can

Table II. The impact of systematic errors for  $\delta \sim 0.1$  on the ability to experimentally determine the resistance regime for both criteria using one-parameter fitting functions. The measured values of the damping parameter  $B$  or  $D$  for the appropriate fitting functions and the large measuring range value  $\alpha$  are also given.

Error type	$B$ and $D$ conv. criterion	$\Delta(\text{RMSE})$ criterion	$B$ or $D$ value ( $\text{s}^{-1}$ )
Equilibrium position error	Work	Work	$\sim(1 + 2\delta)$
Normalization error	Limited	Doesn't work	$\sim(1 + \delta)$
Constant error	Limited	Doesn't work	$\sim(1 + \delta)$

be the difference in the quality of both fits or the observation of varying the measured parameters by gradually integrating additional points at the end of the measurement range. If the determination of the regime is not reliable, we can improve the reliability of the model and the measured damping parameters by including additional parameters. In this way, we can also investigate systematic errors.

## ACKNOWLEDGMENTS

For useful suggestions, the authors thank Professor Dr. Jana Padežnik Gomilšek from the Faculty of Mechanical Engineering, University of Maribor, Slovenia. The authors would also like to thank Professor Dr. Victor Kennedy for English language editing. This research was supported by the Slovenian Research Agency (Grant No. P1-0403).

- <sup>1</sup>M. Kamela, "An oscillating system with sliding friction," *Phys. Teach.* **45**, 110–113 (2007).
- <sup>2</sup>M. J. O'Shea, "Harmonic and anharmonic behavior of a simple oscillator," *Eur. J. Phys.* **30**, 549–558 (2009).
- <sup>3</sup>P. Onorato, D. Mascoli, and A. DeAmbrosis, "Damped oscillations and equilibrium in a mass-spring system subject to sliding friction forces: Integrating experimental and theoretical analyses," *Am. J. Phys.* **78**, 1120–1127 (2010).
- <sup>4</sup>C. L. Ladera and G. Donoso, "Oscillations of a spring-magnet system damped by a conductive plate," *Eur. J. Phys.* **34**, 1187–1197 (2013).
- <sup>5</sup>C. E. Mungan and T. Lipscombe, "Oscillations of a quadratically damped pendulum," *Eur. J. Phys.* **34**, 1243–1253 (2013).
- <sup>6</sup>T. Corridoni, M. D'Anna, and H. Fuchs, "Damped mechanical oscillator: Experiment and detailed energy analysis," *Phys. Teach.* **52**, 88–90 (2014).
- <sup>7</sup>R. D. Peters and T. Pritchett, "The not-so-simple harmonic oscillator," *Am. J. Phys.* **65**, 1067–1073 (1997).
- <sup>8</sup>X. Wang, C. Smith, and M. Payne, "Oscillations with three damping effects," *Eur. J. Phys.* **23**, 155–164 (2002).
- <sup>9</sup>M. I. Molina, "Exponential versus linear amplitude decay in damped oscillators," *Phys. Teach.* **42**, 485–487 (2004).

- <sup>10</sup>G. Flores-Hidalgo and F. A. Barone, "The one-dimensional damped forced harmonic oscillator revisited," *Eur. J. Phys.* **32**, 377–379 (2011).
- <sup>11</sup>G. D. Quiroga and P. A. Ospina-Henao, "Dynamics of damped oscillations: physical pendulum," *Eur. J. Phys.* **38**, 065005 (2017).
- <sup>12</sup>G. Dolfo, D. Castex, and J. Vigué, "Damping mechanisms of a pendulum," *Eur. J. Phys.* **37**, 065004 (2016).
- <sup>13</sup>P. F. Hinrichsen and C. I. Larnder, "Combined viscous and dry friction damping of oscillatory motion," *Am. J. Phys.* **86**, 577–584 (2018).
- <sup>14</sup>R. Hauko, D. Andreevski, D. Paul, M. Šterk, and R. Repnik, "Teaching of the harmonic oscillator damped by a constant force: The use of analogy and experiments," *Am. J. Phys.* **86**, 657–662 (2018).
- <sup>15</sup>G. Falkovich, *Fluid Mechanics* (Cambridge U. P., Cambridge, 2011).
- <sup>16</sup>L. D. Landau and E. M. Lifshitz, *Fluid Dynamics*, 2nd ed. (Pergamon Press, Oxford, 1986).
- <sup>17</sup>N. A. Fuchs and C. N. Davies, *The Mechanics of Aerosols* (Dover Publications, New York, 1989).
- <sup>18</sup>F. F. Abraham, *Phys. Fluids* **13**, 2194–2195 (1970).
- <sup>19</sup>H. Zhe, Y. Kai, X. Fuyong, J. Hai, and S. Qingfan, "Oscillations properties of a simple pendulum in a viscous liquid," *Eur. J. Phys.* **36**, 015011 (2015).
- <sup>20</sup>W. E. Keig, "Velocity dependence of friction on an air track," *Am. J. Phys.* **53**, 1084–1085 (1985).
- <sup>21</sup>R. P. Feynman, R. B. Leighton, and M. L. Sands, *The Feynman Lectures on Physics* (Addison-Wesley, Reading, 1989).
- <sup>22</sup>D. Halliday, R. Resnick, and J. Walker, *Fundamentals of Physics*, 8th ed. (Wiley, Chichester, 2008).
- <sup>23</sup>H. D. Young and R. A. Freedman, *Sears and Zampansky's University Physics: With Modern Physics*, 11th ed. (Addison-Wesley, San Francisco, 2004).
- <sup>24</sup>R. A. Serway, *Physics For Scientists & Engineers*, 3th ed. (Saunders Golden Sunburst Series, Philadelphia, 2004).
- <sup>25</sup>D. C. Giancoli, *Physics Principles with Applications*, 4th ed. (Prentice-Hall International, London, 1995).
- <sup>26</sup>B. R. Smith, Jr., "The quadratically damped oscillator: A case study of a non-linear equation of motion," *Am. J. Phys.* **80**, 816–824 (2012).
- <sup>27</sup>J. R. Taylor, *Introduction to Error Analysis: The Study of Uncertainties in Physical Measurements* (University Science Books, Sausalito, 1997).
- <sup>28</sup>M. Grabe, *Measurement Uncertainties in Science and Technology* (Springer, New York, 2005).
- <sup>29</sup>"Root-mean-square deviation," <[https://en.wikipedia.org/wiki/Root-mean-square\\_deviation](https://en.wikipedia.org/wiki/Root-mean-square_deviation)>.

### MAKE YOUR ONLINE MANUSCRIPTS COME ALIVE

If a picture is worth a thousand words, videos or animation may be worth a million. If you submit a manuscript that includes an experiment or computer simulation, why not make a video clip of the experiment or an animation of the simulation. These files can be placed on the Supplementary Material server with a direct link from your manuscript. In addition, video files can be directly linked to the online version of your article, giving readers instant access to your movies and adding significant value to your article.

See <http://ajp.dickinson.edu/Contributors/EPAPS.html> for more information.